AJAE

Open Access

Vol. 16, No. 2, 2022007, June 2022
doi: https://doi.org/10.5572/ajae.2022.007
ISSN (Online) 2287-1160, ISSN (Print) 1976-6912

Research Article

Modeling of the Calm Situations in the Atmosphere of Almaty

Edige Zakarin[1)], **Alexander Baklanov**[2)], **Larissa Balakay**[1)], **Tatyana Dedova**[1),*], **Kairat Bostanbekov**[1)]

[1)]EcoRisk LLP, 42 Aitiyeva str, Almaty, 050026, Kazakhstan
[2)]World Meteorological Organization (WMO), 7 bis, Avenue de la Paix, BP2300, CH-1211 Geneva 2, Switzerland

***Corresponding author.**
Tel: +7-7017230158
E-mail: dedova3007@gmail.com

Received: 20 January 2022
Revised: 18 March 2022
Accepted: 24 March 2022

ABSTRACT This article addresses modeling of the atmospheric boundary layer of the city of Almaty (Kazakhstan) in stagnant, environmentally unfavorable conditions using WRF Model. The city is located on the northern slope of Trans-Ili Alatau, where the rate of recurrence of calm and low-wind (1–2 m/sec) days reaches about 80%. All simulations were made for a period from 28.11.2016 to 05.12.2016, covering main synoptic situations of the stagnant atmosphere: the extent of Asian anticyclone, higher and lower pressure gradient fields. The model integrated three nested domains with grid sizes 9, 3 and 1 km, respectively. The initial boundary conditions were formed based on ERA5-reanalysis. Subject to the WRF model requirements, the land-use map with a standard USGS set (24 categories) was developed, to which 3 categories of the urban areas were added. The most relevant configuration of parameterization methods was selected: short-wave and long-wave radiation (Mlawer), surface layer (Monin-Obukhov similarity theory), urban area (BEP), boundary layer (Bougeault-Lacarrere), turbulence (Smagorinsky). The article demonstrates that the WRF model adequately reflects fundamental urban atmosphere patterns in the most unfavorable anticyclone periods of the autumn-winter season. It was established that the accuracy of estimates decreases with the transition to weak cyclonic activity. Based on the simulation results and remote sensing data, the territory in question is divided into four climatic zones to which a comparative method was applied; however for a detailed correlative analysis a denser network of meteorological stations is required. Calculations showed that the wind along the Ili river valley prevails in the northern part, regularly changing its western direction to eastern. Near the mountain area mountain-valley wind circulation prevails. The blocking inversion layer has a strong impact. The urban heat islands strongly depend on wind conditions. For example, a nocturnal heat island is cooled by the cold wind flow from the mountains.

KEY WORDS Calm situations, WRF modeling, Mountain-valley wind circulation, Inversion layer, Urban heat island

1. INTRODUCTION

The problem of modeling of the atmosphere of the cities located in the mountain area relates to the task of the highest order of complexity. It is necessary to take into account such factors as highly rugged hilly foothills turning into mountains, dynamically changing thermal regime, complex land-use structure, including urban development. The urgency of this problem relates to the environmental consequences:

the air of such cities is characterized by a high level of pollution caused by frequent recurrence of calm and low-wind conditions and temperature inversions. Almaty belongs to such depressed cities (see section 2.1).

The wide use of WRF (Weather Research and Forecasting) modeling for the cities located in the complex rugged terrain, e.g. Barcelona (Segura *et al.*, 2021), Santiago (Yáñez-Morroni *et al.*, 2018) and Madrid (Diáz-Fernández *et al.*, 2020), determined the objective of this work - WRF model calibration for the conditions of Almaty and its use to analyze atmospheric processes during stagnation periods. Specifically, WRF-ARW (Advanced Research WRF) (Skamarock *et al.*, 2019) model having an effective set of tools allowing choosing microphysical processes parameterization methods relevant to the set objective was used. In addition, this model is compatible with the model of transfer and chemical transformation of pollutants - WRF/CHEM. The results of the first stage of these studies were published in the work (Zakarin *et al.*, 2021a).

The sections of this work focus on the adaptation of the WRF model to the air basin of Almaty and the analysis of modeling results. The background information about the city and its air basin, described in sub-section 2.1, became the basis for the formation of the input information package (sub-section 2.2), choice of an optimal configuration of parameterization methods, including numerical experiments to determine the model spin-up period (sub-section 2.3). The analysis of modeling results and field data is broken up in two sections: sections 3 and 4, dealing with wind and temperature conditions respectively. The whole analysis is based on the area climatic zoning and binding of the existing meteorological stations thereto (sub-section 3.1). It allowed comparing modeling results with field data for each zone separately (sub-section 3.2). The result of wind conditions analysis was mapping of the complex local winds structure: mountain-valley wind circulation (MVWC) and regional transport along the mountain ridge and the Ili River valley (sub-section 3.3). In section 4 the thermal conditions pattern is broken into comparative analysis of thermal conditions of different climatic zones (sub-section 4.1), reviewing variation with time of temperature of the surface layer in the locations of meteorological stations (sub-section 4.2), formation and development of the inversion layer (sub-section 4.3), playing an important role in suppressing vertical exchange and occurrence of atmospheric air pollution, and studying the urban heat island (UHI) given local winds impact during day and night (sub-section 4.4).

2. METHODOLOGY

2.1 Description of the Study Area

Almaty is the largest city in the Republic of Kazakhstan (43°15′N 76°54′E), with a total area over 680 square kilometers. The population of the city comprises over 1.9 million people. The main climatic factor for Almaty is its geographic position in the foothills of the northern slope of the Trans-Ili Alatau range. Most of the city is situated on the comparatively flat-sloped surface with a gradient of 1–2 degrees northbound. However, the recent increase of the urban area shifted the city limits towards the mountains where own microclimate zones are formed, but the most part of the population live in the former piedmont districts. The mountainous area, the height of which reaches 4–5 km, and channeled gorges of such rivers as Bolshaya Almatinka and Malaya Almatinka rivers, Yesentai river etc., form wind, thermal and turbulent conditions of the air basin of the city.

Regardless of the fact that the city is open in the northern and northwestern directions, the recurrence of calm conditions (wind velocity is up to 1 m/sec) in summer is estimated to be 71%, in winter it reaches 79% (https://ecogosfond.kz/wp-content/uploads/2018/03/PRT-2017_RUS-almaty.pdf, Vilesov, 2010). Such unfavorable in terms of atmospheric air pollution conditions are formed mainly under the influence of the Asian (Siberian) anticyclone in winter and thermal depression in the territory of Kazakhstan in summer (Akhmetzhanov and Shver, 1986). In calm conditions the whole system of local winds is formed in the atmosphere of the city under the influence of orographic and thermal heterogeneity. These are slope winds, mesojets from gorges, circulations around the urban heat island and MVWC.

Researches performed by Helmholtz (Helmholtz, 1963), revealed MVWC principal features on the northern slopes of Tien Shan, where Almaty is situated. As shown in this work, in calm conditions in the surface layer MVWC daily cycles are formed during the phases of katabatic flow (mountain breeze) and anabatic flow (valley breeze), in addition, counter-flows are formed in the upper layers of the atmosphere.

It should be noted that the MVWC pattern depends heavily on the season. So, in summer the circulations are more prominent due to a considerable temperature gradient: all phases are more clearly traced and higher airflow velocities are observed. In winter, the mountain breeze flows a greater part of the day for the account of

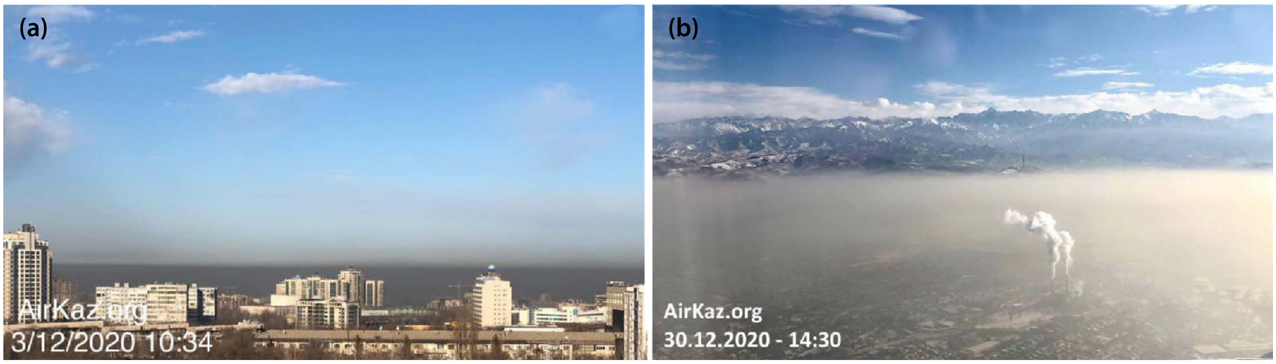

Fig. 1. Air pollution of Almaty in the inversion layer, blocking vertical exchange; (a) morning smog in the northern part of the city, (b) daytime smog covers the entire city.

shorter daylight hours and a low level of solar radiation.

Such processes of generation and development of the inversion layer play an important role in all basic phases of MVWC full daily cycle:

- Nocturnal phase: katabatic flow from the mountains is slowed up in the foothills and urban area and is accumulated in the form of a "lenses" of cold air forming powerful surface inversion.
- Morning phase: the underlying surface and adjacent air layer are warmed-up under the influence of solar radiation. The inversion layer blocks vertical flows, therefore warm air starts flowing up the mountain slope, hence the valley breeze is formed.
- Daylight phase: with the increase of radiation flows, a part of energy creates valley breeze, and another part - warms up lower layers of inversion revealed by rising of the inversion layer limit.
- Evening phase: valley breeze deceleration, generation of katabatic flow and beginning of formation of new lenses of cold air.

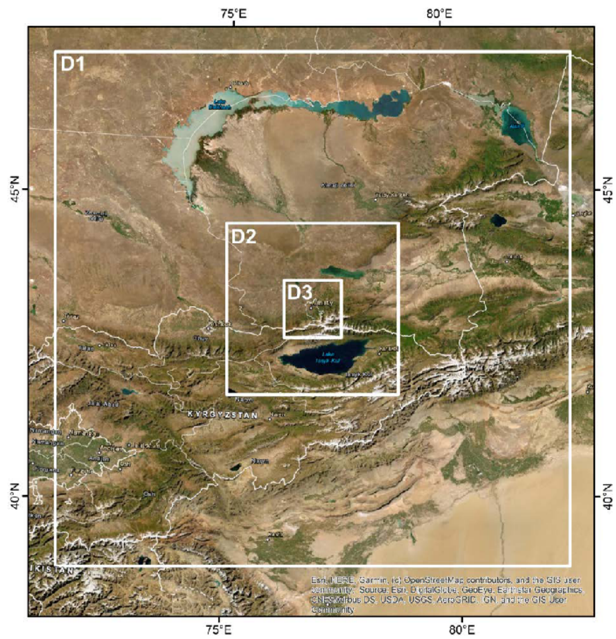

Fig. 2. Nested domain system for the study area.

Such dynamics of the inversion layer is clearly identified in the photos as a dirty air layer, blocked by the temperature inversion in the lower atmospheric layers. Moreover, in the morning hours, smog is formed in the lower northern part of the city (Fig. 1a). At daytime, the inversion layer rises above buildings, and smog covers the entire city (Fig. 1b).

2.2 Research Methods and Input Data

For WRF meteorological modeling (Skamarock *et al.*, 2019) three Lambert conic domains were formed, which configuration is shown in Fig. 2. The first domain D1 has a linear grid cell size of 9 km, the second D2 - 3 km, and the third domain D3 - 1 km. All three domains contain 100 nodes from west to east and 100 nodes from south to north. In vertical extent, 38 levels are used, including 22 levels in the lowest 190-meter layer. A vertical step of 5–10 m in the lower (urban layer) is determined by BEP (Building Environment Parameterization) (Martilli *et al.*, 2009, 2002) model estimating energy exchange among urban structures.

For the purpose of informational support to the WRF model there was developed a geodatabase containing the city cartographic base (street and road network, build-

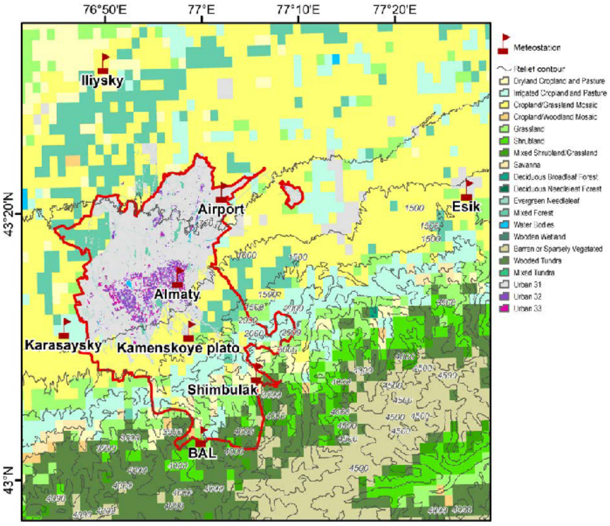

Fig. 3. Land-use map for Almaty.

ings, parks, water reservoirs and enterprises) and Aster GDEM (Global Digital Elevation Model) (https://lpdaac.usgs.gov/news/global-data-explorer-gdex-has-been-retired/).

Based on the geodatabase, there was developed a land-use map (Fig. 3) for the multi-layer urban canopy model BEP, where 3 categories of urban area were added to the standard USGS (United States Geological Survey) set (24 categories) (Martilli *et al.*, 2009):

- Low Intensity residential (Urban 31). This class includes built-up areas with a high vegetation coverage percentage and a low population density, i.e. single-family housing units (one-two-storey structures). Vegetation can occupy from 20 to 70 percent of the canopy.
- High Intensity residential (Urban 32). This category includes multi-storey housing development with a high population density (3–6 storeys). Moreover, vegetation covers less than 20 percent of the canopy.
- Commercial, industrial structures (Urban 33). This category includes multi-storey (over 7 storeys) residential and commercial structures.

Subsequent studies plan to detailise the urban map using the LCZ (local climate zone) classification scheme of the WUDAPT (World Urban Database and Access Portal Tools) project (https://www.wudapt.org/).

Based on the open database of RSE KAZHYDROMET (http://93.185.76.134/), containing synoptic maps of different levels, calm and low-wind conditions for a period from 2015 through 2017 were identified. The result of the analysis showed that such conditions occur in five synoptic regimes: Asian anticyclone wedge, low-gradient field (LGF) of high pressure, LGF of low pressure (in summer - thermal depression, in winter - extensive cyclone trough with a center in the north of the Urals) and warm cyclone sector.

All estimates in this work are made for a period from 28.11.2016 to 05.12.2016. First 6 days of this period (28.11–03.12) the synoptic condition "Asian anticyclone wedge" continued, which with the advent of warm air invasion changed to high pressure LGF (02.12) and low pressure LGF (03.12) with rain precipitation at the end of the period (04–05.12). Initial and boundary conditions were determined according to the ERA5 reanalysis database (https://confluence.ecmwf.int/display/CKB/ERA5).

The analysis of modeling results has used aerological (sounding) observation data, accumulated in the database of the University of Wyoming (https://weather.uwyo.edu/upperair/sounding.html), and meteorological observation data from the "Weather for 243 countries of the world" database (https://rp5.kz/docs/about/en). Only 8 meteorological stations included into the WMO network and presented in the above database are located in Almaty and its environ: Iliysky (№36883, 608 m a.s.l.), Esik (№36885, 1,008 m a.s.l.), Airport (UAAA, 673 m a.s.l.), Almaty (№36870, 848 m a.s.l.), Karasaysky (№36871, 800 m a.s.l.), Kamenskoye Plato (№36875, 1,300 m a.s.l.), Shimbulak (№36873, 2,300 m a.s.l.) and Big Almaty Lake (BAL) (№36879, 2,501 m a.s.l.) (Fig. 3).

2.3 Adjustment of the WRF Model to the Atmospheric Conditions of Almaty

The problem of WRF model adjustment to the complex mountainous area attracts many scientists (Siuta *et al.*, 2017; Jiménez and Dudhia, 2013; Arnold *et al.*, 2012). This article uses the experience of WRF modeling of mesometeorological processes in California Central Valley mountain range (Bao *et al.*, 2008; Michelson and Bao, 2008) and the air basin of Salt Lake City (Nehrkorn *et al.*, 2013) in anticyclone periods. Besides, the experience of adjustment of WRF model to Kyrgyzstan mountain region (Isaev *et al.*, 2017, 2015; Isaev and Aniskina, 2015) located in the same mountain range as the city of Almaty was also important.

The optimal configuration of parameterization methods was selected based on the experience of the above works and a series of trial simulations. The selection criteria were statistical characteristics of the deviation of modeling results from field data of the specified meteorological stations. Moreover there were used mean, absolute and root-mean square deviations of simulations of wind temperature, velocity and direction (Jiménez and Dudhia, 2013; Wilks, 2011).

The following configuration of parameterization methods, selected according to the minimal sum of the said deviations, was used: 6 component cloud microphysics spectral method (Lim *et al.*, 2004), Mlawer parameterization modified by short-wave and long-wave radiation (Iacono *et al.*, 2008), surface layer according to Monin-Obukhov similarity theory (Monin and Obukhov, 1954) outside the city and BEP (Building Environment Parameterization) parameterization (Martilli *et al.*, 2002) for the urban area, Bougeault-Lacarrere parameterization of the boundary layer (Bougeault and Lacarrere, 1989), Kain-Fritsch convective parameterization (Kain and Kain, 2004) and Smagorinsky 2D turbulence parameterization (only for horizontal diffusion) (Skamarock *et al.*, 2019).

A specific attention was paid to the comparative analysis of single-layer Urban Canopy Model (UCM) (Kusaka and Kimura, 2004) and multi-layer BEP model (Martilli *et al.*, 2002). The analysis results demonstrated that BEP 3D diffusive model, built on basic microphysical processes in the layer of urban development and underlying layer of the urban relief, is a good reflection of the impact of the infrastructure of Almaty on local meteorological processes in the stagnant conditions. It can be illustrated by Fig. 4, showing curves of temporal changes of wind velocity at the height of 10 meters, measured by the Almaty meteorological station and intended for BEP and UCM models. It can be seen that BEP model reflects the process of air flow diffusion in the urban canopy and dense urban area better than UCM model. Also, it should be noted that BEP model allows modeling such essential phenomena as inversion layer and urban heat island (UHI) dynamics.

The following series of trial simulations relates to determination of a spin-up period for the model configured based on parameterization methods. The results of modelling are shown below (Fig. 5) in the form of time-temperature curves in the selected grid cell in the airport vicinity. The curves correspond to different (with 6-hour shift) initial moments. Comparison of a series of model runs showed that the spin-up time comprises from 24 up to 27 hours. According to this conclusion, a period from

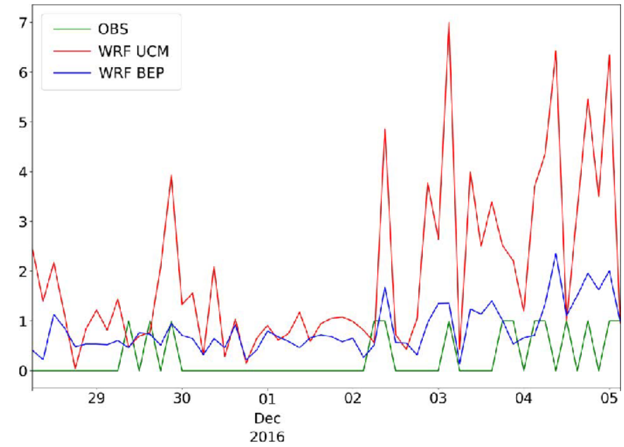

Fig. 4. Comparison of wind velocity observations at the Almaty meteorological station with the modelling results by the UCM and BEP models.

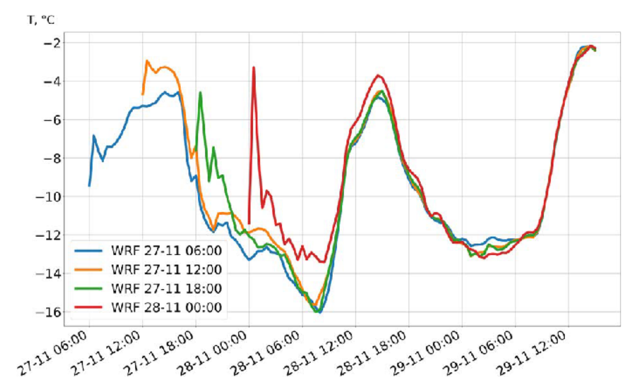

Fig. 5. Time-temperature curves for the airport area, calculated to determine the time of model spin-up; color lines correspond to different moments of the beginning of simulation.

06 hours 27.11 was excluded from consideration, and the subsequent analysis was performed from 09 hours (local time) 28.11.2016.

3. RESULTS AND DISCUSSION: WIND CONDITIONS

3.1 Climatic Zones of the Underlying Surface

Unfortunately, the sparse network of meteorological stations located in Almaty and its environ is not capable to reflect a complex structure of local fields of meteorological elements. Moreover, observations are performed only every 3 hours (except the meteorological station located at the Airport), the accuracy of wind velocity measurements does not exceed 0.5 m/sec, and these data are rounded-off to whole-number values. It causes certain restrictions on the opportunities of critical analysis of the modeling results. Based on the altitudinal zonation of the mountain area, the area of interest, considered in this study, is divided into four climatic zones with code names: high mountain range, middle mountain range, the city and the steppe, and were selected meteorological stations characterizing these zones. Based on it, the information from five meteorological stations: Shimbulak, Kamenskoye Plato, Almaty, Airport and Iliysky was used to compare the results of simulation with observation data. The Airport meteorological station was selected for the analysis of the processes in the buffer area between the city and the steppe. In addition, more frequent (every half an hour) and reliable measurements are made there, ensuring flight safety. First four stations are located in the zone affected by the Malaya Almatinka River gorge, while the Iliysky meteorological station is located in the northern flat area where the latitudinal transport along the Ili River valley plays the main role.

3.2 Analysis of Wind Conditions Based on Observations and Modeling Results

A series of subsequent figures illustrate wind conditions in the surface layer in different zones, as well as the capability of the model to adequately describe these processes. Measured and calculated data for all meteorological stations, except for the high mountain station Shimbulak, characterize wind in the period of anticyclone as light, variable and periodically gusting wind. With the advent of the subdued cyclone the amplitude of wind fluctuations, especially in the undeveloped areas, increases. Moreover, in the period of anticyclone modeling results correspond well to observation data, simulation error increases during synoptic situations of high and low pressure LGF. These common patterns are superimposed by the specifics of the underlying surface in each zone.

The Shimbulak meteorological station is located in the mountains at the altitude of 2,300 m, and, respectively, measurement data characterize wind as gusty with large variations from 0 to 10 m/sec. Given the wind rose, the prevailing wind is the westward slope wind. As expected, observation and simulation results do not correspond to each other (Fig. 6). Probably, modeling of meso-meteorological processes in complex mountainous systems requires the solution of a larger complex of tasks, from increasing the density of the numerical grid to development of new parameterization methods.

Unlike the Shimbulak meteorological station, the Kamenskoye Plato meteorological station is located in the foothills of the high mountain range on the relatively flat area (plateau). Such position of the station reduces simulation errors, related to the sparse mountain numerical grid cells of 1 sq. km. Hence, the modeling results reflect well the microclimate of this zone; it is supported by their correspondence to the measured wind velocities both by value and by direction (Fig. 7). Regression curves, drawn up based on observation and modeling data demonstrated that the modeling results reflect well dynamics of wind velocity variation in the period of anticyclone and high and low pressure LGF.

The wind rose diagram (Fig. 7b) shows that at the middle altitudes the wind conditions are determined by the mountain breeze (southern wind), the velocity of this wind reaches 3–4 m/sec, and daily anabatic flows subside (northern wind). The mountain-valley wind cir-

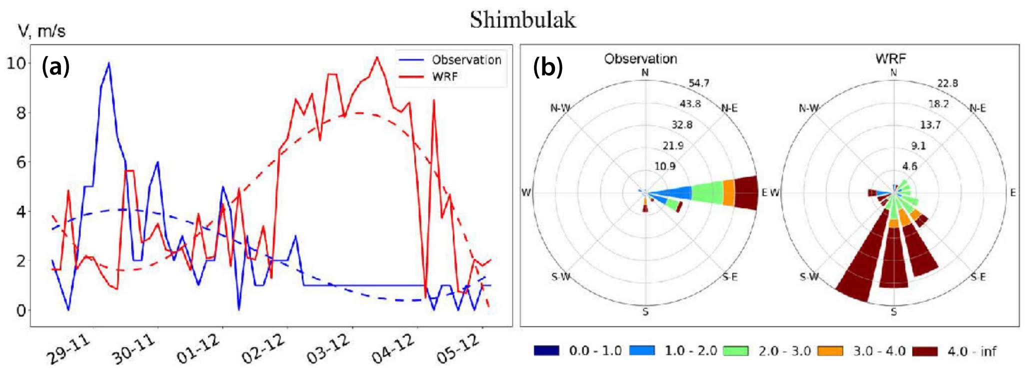

Fig. 6. Dynamics of wind velocity changes during 7 days, beginning from 28.11.2016 09:00 and the wind rose diagram for the Shimbulak meteorological station. Dotted lines correspond to regression curves drawn up by the least-square method of the 3rd order.

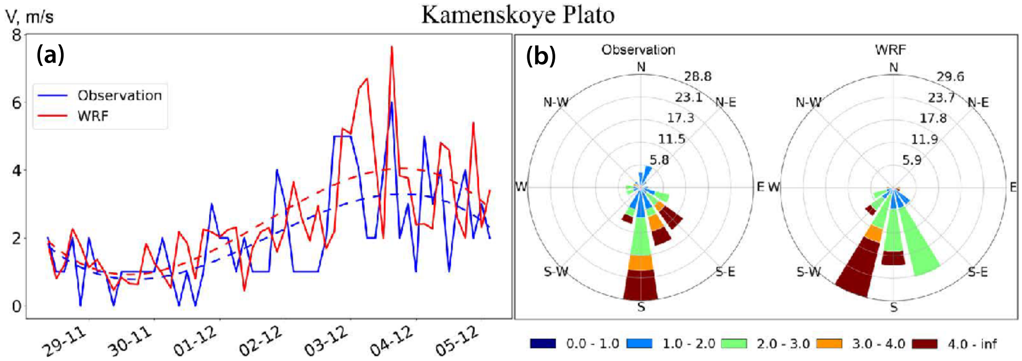

Fig. 7. Dynamics of wind velocity changes during 7 days, beginning from 28.11.2016 09:00 and the wind rose diagram for the Kamenskoye Plato meteorological station.

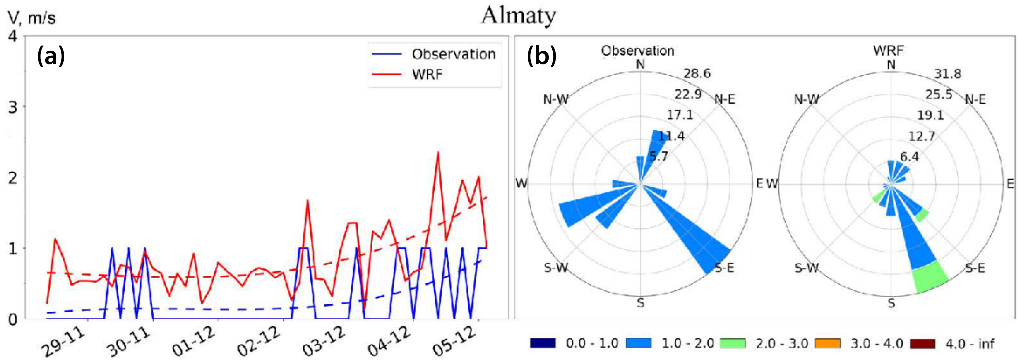

Fig. 8. Dynamics of wind velocity changes during 7 days, beginning from 28.11.2016 09:00 and the wind rose diagram for the Almaty meteorological station.

culation pattern in this zone can be traced in more detail on the vertical wind flows profile (see sub-section 3.3). Thus, WRF model in the Kamenskoye Plato meteorological station forecasts well wind value and direction during synoptic stagnation periods.

Comparison of the wind velocity observed and calculated data in the vicinity of the Almaty meteorological station is given in Fig. 8a. Unfortunately, the measurement error (0.5 m/sec) and the procedure of results rounding off to whole-number values; reduced to 0 and 1 m/sec the whole spectrum of wind velocity fluctuations within the range from 0 to 1.5 m/sec. Model simulations also demonstrate light (from 0.5 to 1 m/sec) and variable wind in anticyclone conditions and slight uptick (up to 2 m/sec) in speed with arrival of the warm front. The wind rose diagram (Fig. 8b), constructed based on measurement data, demonstrates that within the simulation period prevailing light variable northwestward wind was observed, which is consistent with the modeling data. However, comparison by wind velocity indicates that the model does not fully account for wind flow stagnation in the dense urban area. Probably, it is necessary, based on the experience of the study (Brousse *et al.*, 2016), to use a denser numerical grid and a more detailed urban development plan or to adjust WRF model with BEP parameterization using CIM (Canopy Interface Model) model (Mauree *et al.*, 2018).

The Airport meteorological station is located in the open space similar to a runway; the grid cell partially includes structures adjoining the meteorological station. It relates to wind velocity difference: the observed wind is less stagnated and is stronger (from 0 to 3 m/sec) than the simulated wind (from 0 to 2 m/sec) (see Fig. 9a). Regression curves (dotted line) also reflect this fact: the measurement curve is above the calculation curve. With the arrival of the warm front both observed and simulated wind velocities increase to 7–8 m/sec and 4–5 m/sec, respectively.

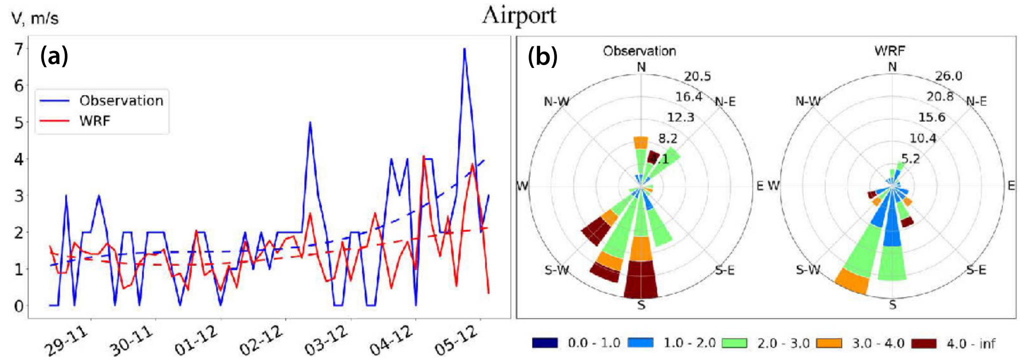

Fig. 9. Dynamics of wind velocity measurements during 7 days, beginning from 28.11.2016 09:00 and the wind rose diagram for the Airport meteorological station.

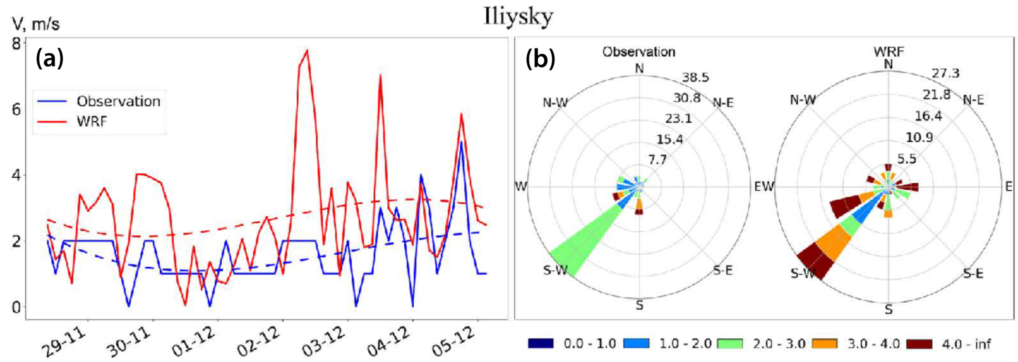

Fig. 10. Dynamics of wind velocity changes during 7 days, beginning from 28.11.2016 09:00 and the wind rose diagram for the Iliysky meteorological station.

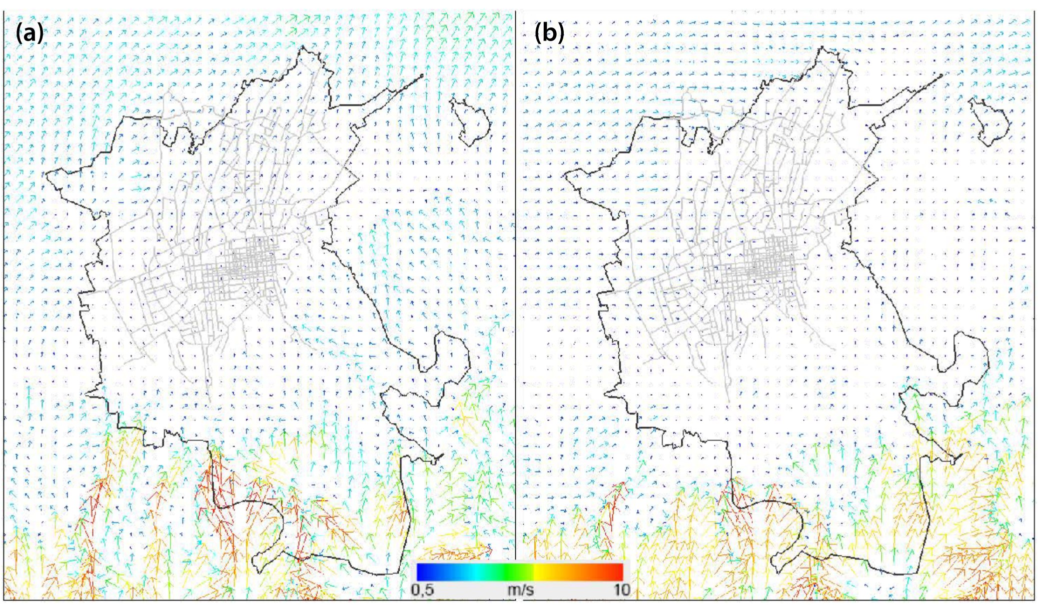

Fig. 11. Wind fields in the surface layer of Almaty and its vicinity on 29.11.2016, (a) 00:00, (b) 12:00. A road network was given prominence to identify the city residential area.

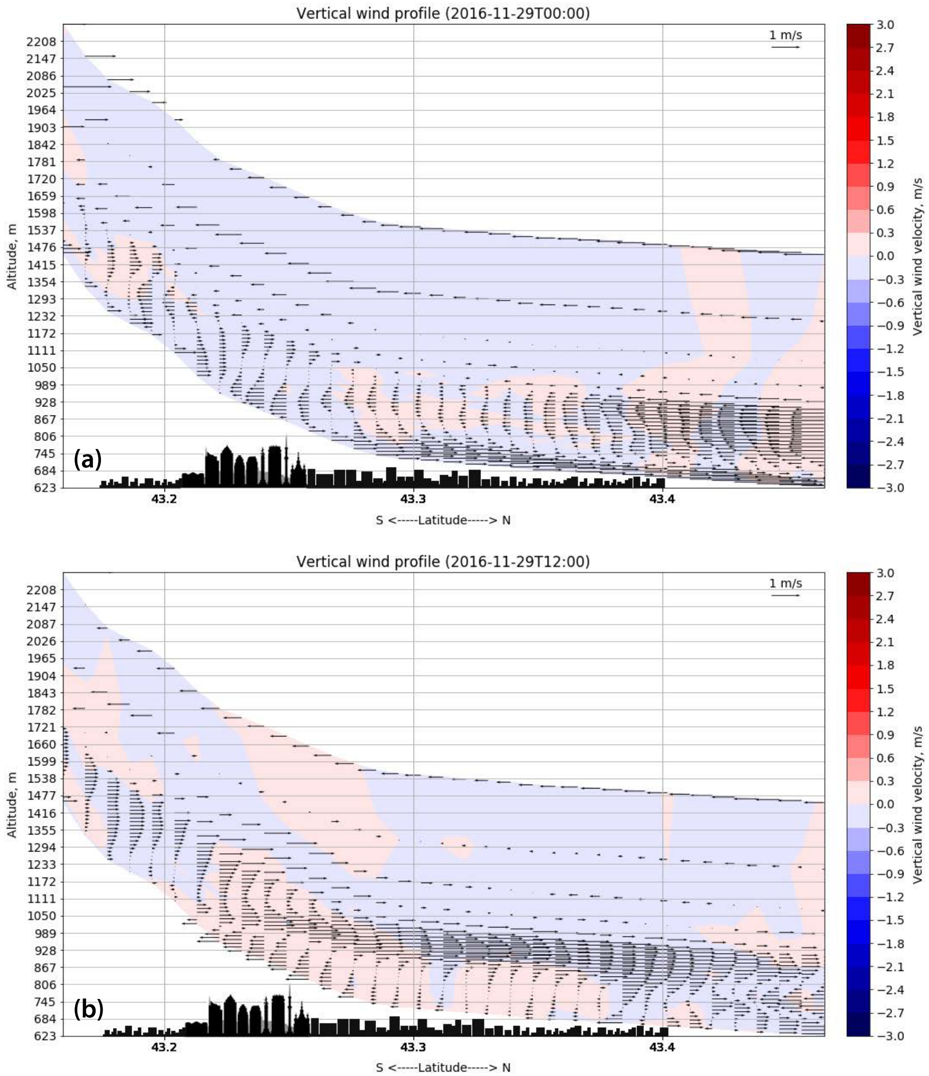

Fig. 12. Vertical section of the wind field along the line South-North, passing through the Almaty meteorological station. The arrows show a horizontal $\boldsymbol{v}$-component of the wind, and color shows the vertical component $\boldsymbol{w}$. There are presented nocturnal ((a) 00:00) and daytime ((b) 12:00) wind profiles for 29.11.2016.

Comparison of wind rose diagrams in the area of this meteorological station (Fig. 9b) shows close coincidence by prevailing wind direction (northward and north-northeastward). This direction corresponds to the wind breeze, which is formed in the Malaya Almatinka River gorge and reaches the city suburbs.

The Iliysky meteorological station is located on the plain in the northern part of the study area, where the air circulation is determined by the regional processes. Among them there is distinguished the Shilik mountain breeze with a speed of up to 10 m/sec, forming in the gorge near the headwater of the Shilik River and blowing along the Ili valley. Observations show (Fig. 10) that this wind blows from southwest and reaches the meteorological station significantly weakened, up to 2 m/sec during the anticyclone period. With the advent of warm intrusion, the wind becomes stronger with gusts up to 3–4 m/sec. Comparison of simulation and observation data at this station demonstrated that the model overestimates wind velocity, but correctly determines the prevailing directions of airflows. It should be noted that Shilik and other regional airflows, forming along the Trans-Ili Alatau ridge intensify aeration in the northern part of the city during environmentally unfavorable stagnant periods.

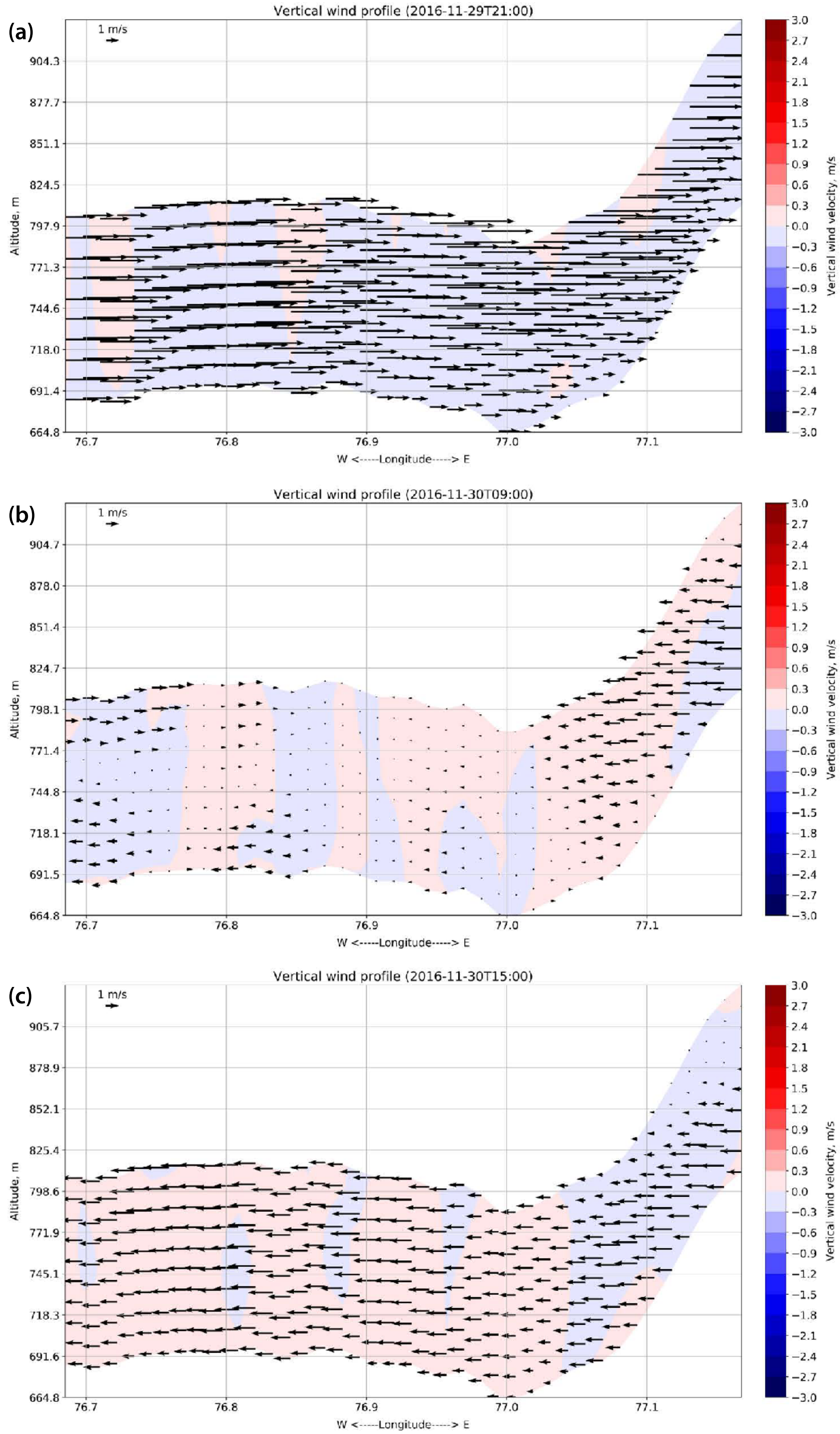

Fig. 13. Wind profiles along the East-West line passing through the Airport meteorological station, (a) 21:00, 29.11, 2016, (b) 09:00, 30.11, 2016, (c) 15:00, 30.11, 2016. The arrows show a horizontal $\boldsymbol{u}$-component of the wind velocity, and color shows a vertical $\boldsymbol{w}$-component.

3.3 Analysis of Wind Fields Based on Modeling Results

The key factors determining a high level of pollution of the atmosphere of the city during anticyclone periods, when no precipitation occurs, are wind and turbulence conditions. Fig. 11 illustrates a typical picture of the surface wind field in stagnant conditions.

As was to be expected, a complex wind picture is observed in the mountains with a large velocity gradient. However, the foothill areas where the city is situated are located in the wind shadow, moreover urban development restrains wind flows. Thus, low-wind and calm weather is established in the city, moreover this condition continues within the whole anticyclone period.

A more detailed picture of the structure of these light air flows is demonstrated by the vertical section of the wind field (Fig. 12). Here for clarity ***y***-wind components - ***v*** are mapped. Based on the figure (Fig. 12a) it is clear that the nocturnal drainage wind is stronger in the northern part of the city closer to the ground surface, while the counter-flow is formed in the upper atmospheric layers. In the south, steep mountainous slopes destroy this circulation mesh. Probably, the circulation at the border of the urban heat island also contributes to it. As the result, wind velocity drops, and aeration decreases. As was to be expected, the daytime anabatic up-flow (Fig. 12b) has lower speeds, less than 1 m/sec.

During stagnation periods, the air circulation along the Trans-Ili Alatau mountainous ridge also affects wind conditions. These sub-latitudinal flows are the manifestation of the regional processes, forming near the mountainous area. The results of modeling of these flows are given below (Fig. 13) in the form of vertical section of the wind field in the East-West plane through the cell where the Airport meteorological station is located.

It should be noted that the latitudinal transport plays a prevailing role in the northern part of the city. Its characteristic property is a regular change of wind directions from eastern to western and vice versa from western to eastern. Fig. 13 consequentially shows examples of airflows from west to east (Fig. 13a), the process of direction change (Fig. 13b) and transport from east to west (Fig. 13c). In addition, based on the figures, it is seen that this wind does not induce counter-flows in the upper layers, and it has low velocities in the surface layer.

4. RESULTS AND DISCUSSION: THERMAL CONDITIONS

4.1 Thermal Conditions of Climatic Zones in the Underlying Surface

Zoning, specified in section 3, manifests well on daytime thermal satellite images (Fig. 14a). As long as the altitude increases, a cold mountainous zone is replaced with the warmed-up belt of middle mountainous range, further there follows the urban heat island (UHI) and the cool steppe zone. The satellite image correlates well with the temperature field constructed based on the WRF modeling results (Fig. 14).

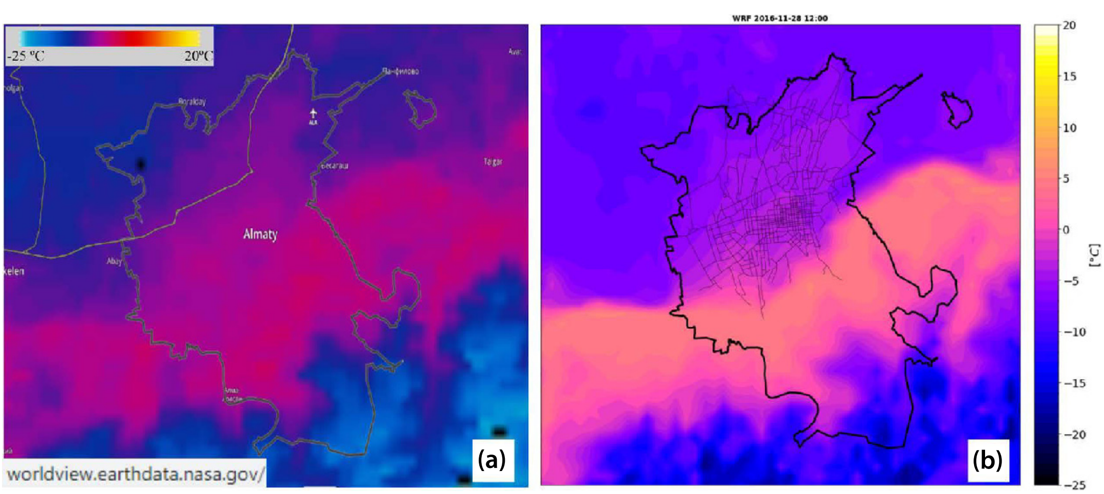

Fig. 14. Thermal fields in the city of Almaty and its vicinity. (a) ground surface temperature based on Terra/MODIS satellite data, 28.11.2016, daylight survey; (b) temperature of the ground surface atmospheric layer by the WRF model, 28.11.2016/12:00.

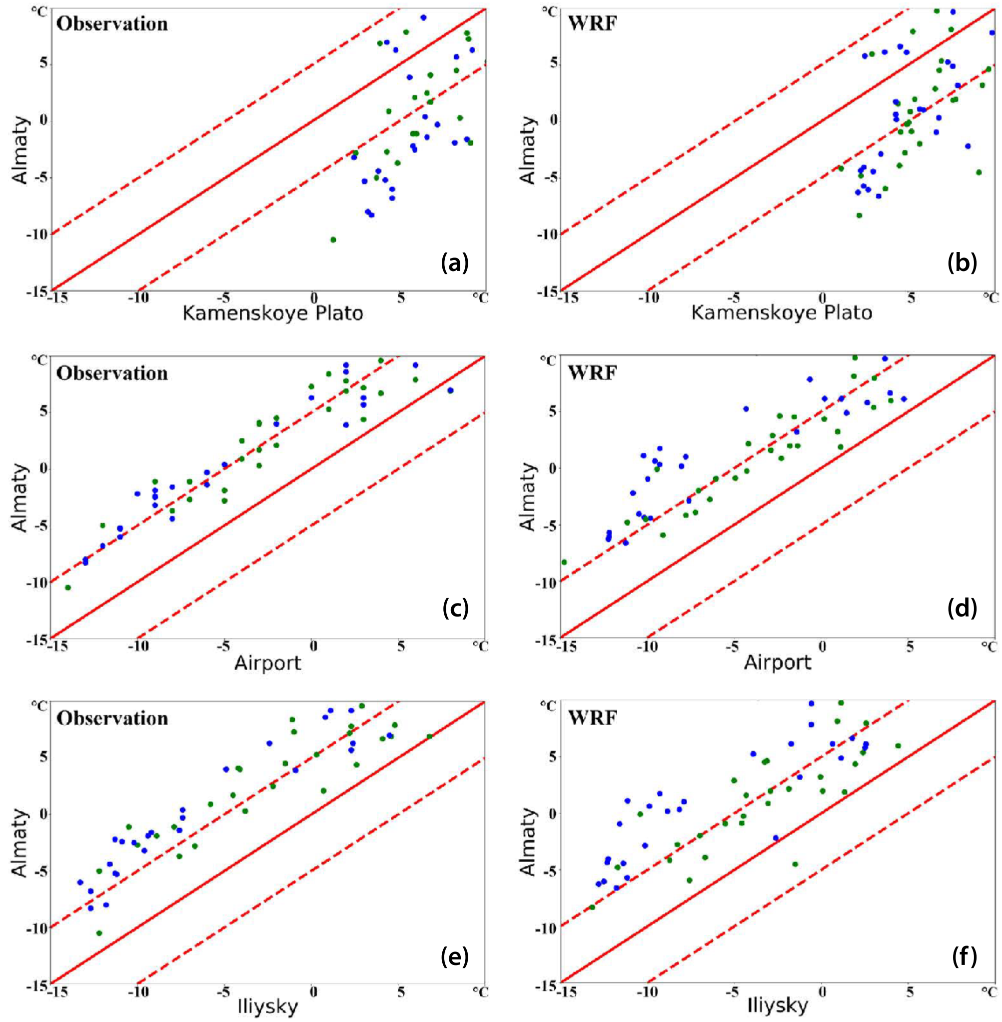

Fig. 15. Correlation of the temperatures of Almaty - Kamenskoye Plato, Almaty - Airport, Almaty - Iliysky. Red dotted lines correspond to the temperature difference of +5 and −5°C. Dots map observations taken 8 times per day during the entire test period from 28.11.2016 09:00 through 05.12.2016 05:30; blue dots correspond to nighttime (from 21:00 through 6:00); green dots - daylight time (from 9:00 through 18:00).

Meteorological data gives an opportunity to perform a qualitative assessment of thermal conditions in different zones. Fig. 15 shows temperature correlation dependence in the center of the city (at the Almaty meteorological station) on similar data at the meteorological stations in other zones.

Difference of thermal conditions in Almaty and the adjacent mountainous area is well illustrated by the correlation between temperature observations at the Almaty and Kamenskoye Plato meteorological stations (Fig. 15a). As can be seen in the picture, the temperature of the middle mountainous range is higher than in the city during most of the time, moreover, warming-up changes within a wide range from 0 to 10°C. Rare moments when the temperature in the city is higher than in the mountains fall on the periods of light cloud cover appearing at the end of the modeling period in case of warm intrusion. Therefore, the radiation heating due to the exposition of the slopes in this zone exceeds the UHI thermal effect. Similar results demonstrate modeling results (Fig. 15b).

UHI manifests when comparing temperatures in the city and in the northern suburb zone named above as the steppe zone. The thermal conditions of this extensive zone are characterized by the observations at the Airport and Iliysky meteorological stations. As shown in Fig. 15c and Fig. 15e heat in the urban area accumulates with a

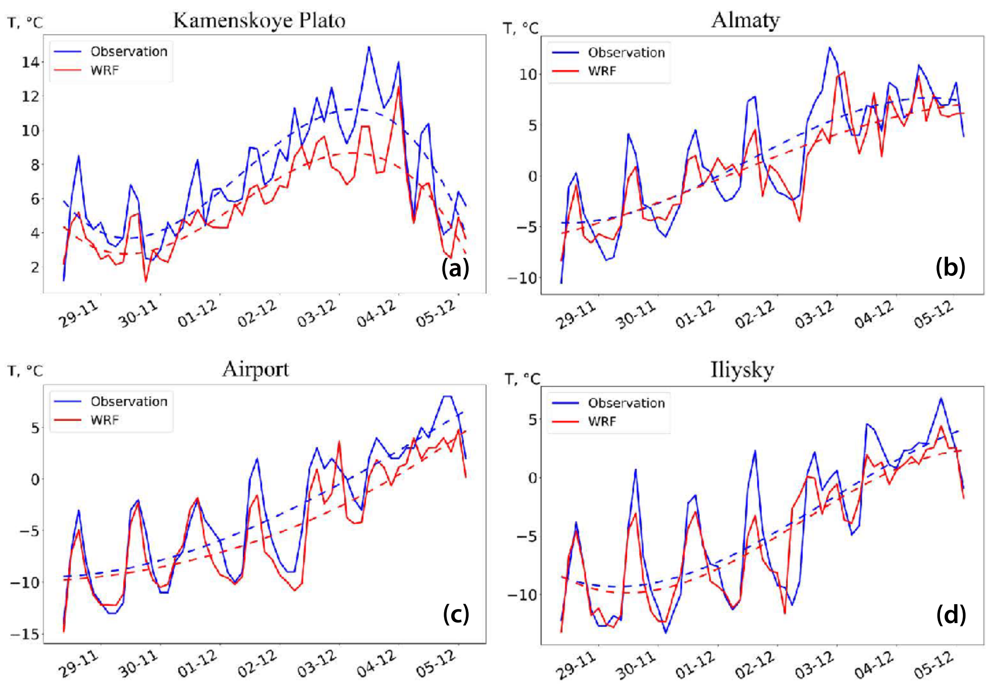

Fig. 16. Time variation of temperature at the meteorological stations during the entire period in question. Blue line - observations, red line - model; (a) Kamenskoye Plato, (b) Almaty, (c) Airport, (d) Iliysky.

mean overheating of 5°C. Modeling results (Fig. 15d and Fig. 15f) also point out to the UHI effect, but the nocturnal simulation points have dispersion towards greater overheating. Main UHI peculiarities of the city of Almaty according to WRF modeling data are discussed in section 4.4.

4. 2 Dynamics of Temperature at the Meteorological Stations

Dynamics of thermal conditions in the surface atmospheric layer (Fig. 16) reflects air daylight warming-up and nocturnal cooling, and the synoptic process of warm intrusion, replacing the anticyclone conditions. Good correlation of simulation and observation data continues within the entire anticyclone period from 28.11.2016 through 01.12.2016. With the advent of weak cyclone activity, the error of thermal process modeling increases, but the process of warm intrusion is captured correctly. On Kamenskoye Plato the arrival of the warm front is followed by light clouds; it results in the decrease of radiation heating and respectively temperature.

4. 3 Inversion Layer Dynamics

The peculiarity of the atmosphere of Almaty related to the formation of the inversion layer blocking the vertical exchange is also reflected in modeling results. Fig. 17 shows the dynamics of the vertical profiles of potential temperature and the v-component of the wind velocity by the y-coordinate, directed from south to north, i.e. from the mountains to the valley. As can be seen in the figure, in the morning at 6:00 and 9:00 of local time the nocturnal conditions retain: cold air lies close to the surface (surface inversion) and the wind in the lower atmospheric layers are practically absent. By 12:00 the sun heats up the surface and an elevated inversion is formed that inhibits vertical exchange. Therefore, air heated near the surface partially destroys the inversion, shifting its border upward, partially slowly rises upward to the mountains along the ground surface forming anabatic airflow. It should be noted that this process is observed in the atmosphere of the city as the flow of polluted air upward and towards mountains (Fig. 1). At 15:00 the process intensified, the lower border of the inversion layer rose by 150–200 meters, the mountain upward breeze increased to 1.5–2 m/sec. At the sunset at 18:00 the earth cools, the anabatic wind rises to higher atmospheric layers, and the katabatic flow begins to form near the surface.

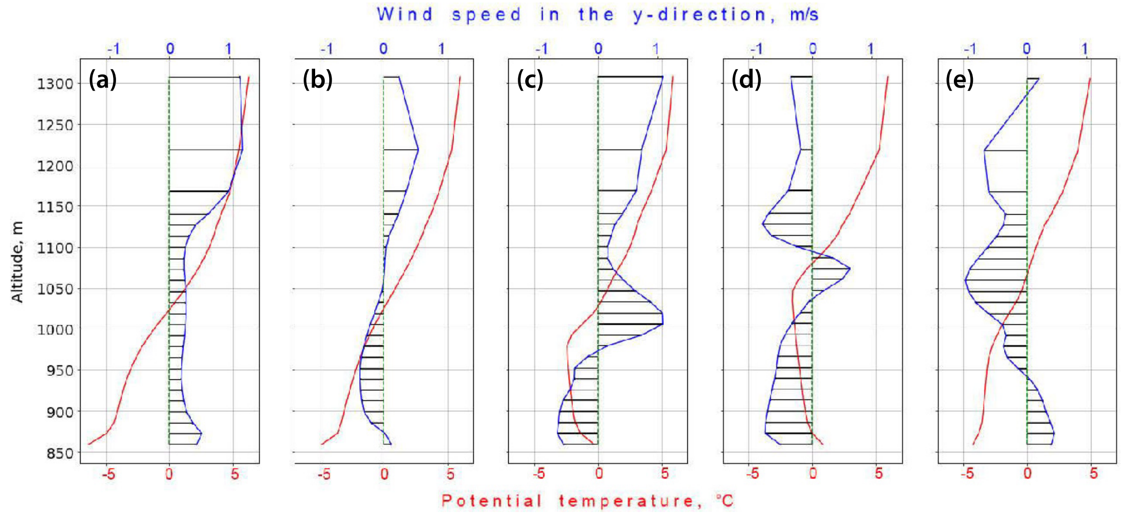

Fig. 17. Dynamics of the vertical profile of potential temperature (red lines) and the v component of the wind velocity during daylight time on 29.11.2016; (a) 06:00, (b) 09:00, (c) 12:00, (d) 15:00, (e) 18:00.

4.4 Urban Heat Island Pattern

The main peculiarities of the climate of the city are characterized by the urban heat island forming as the result of anthropogenic heating of the blocks of buildings, roads and other infrastructure objects (Oke *et al.*, 2017). The heat island of Almaty has a number of defining characteristics related to its location on the tough terrain.

Modeling results allow mapping of the heat island in different conditions and use it as an indicator of the processes forming the climate of the city. In this work, the map of the heat island was calculated as a difference between the thermal field, accounting for the urban area, and similar field regardless the city. In the latter case, simulations were performed, based on the land-use map, where the urban land was replaced by agricultural land (arable lands and pastures).

The analysis was based on the anticyclone period from 28.11.2016 through 01.12.2016, when, according to synoptic maps, warm intrusion did not reach the air basin of the city. For filtering temperature fluctuations there were selected periods when daylight (from 11:00 to 16:00 hours) and nocturnal (from 23:00 to 04:00) conditions are set. Respectively, daylight and nocturnal heat islands were calculated by time averaging. Fig. 18 demonstrates the modeling results for four days of the anticyclone period.

The results of comparative analysis of the temperature fields show that the daylight heat island with a temperature difference of 3–4°C covers the entire residential sector, moreover, the northern part of the city gets more heat, while the part of the city close to the mountains gets less heat, and on the steep foothill slopes during the first two days of anticyclone cold islands formed (Fig. 18a, Fig. 18c). Probably, their appearance relates to the circulation at the border of the heat island, where warmed-up air rising is compensated by a cooler counterflow. It should be noted that in this district, the anabatic airflow and slope winds participate in the formation of the wind conditions, but their origin does not relate to the urban area. During two subsequent days, the anticyclone weakens and the heat island intensity drops (Fig. 18e and Fig. 18g).

At night, a greater role is played by the katabatic flow. Outside the city, it cools the whole territory well. The urban area, depending on its intensity, warms up the air and, as the result of it, a weak heat island appears in the north of the city, the island is more intensive in the southern part with dense and multi-storey buildings: the temperature difference reaches 2–3°C (Fig. 18b and Fig. 18d). Weakened anticyclone causes intensification of the latitudinal transport in the northern part of the city. It blows out warm air from the urban area, reducing and weakening the heat island. In this background the vegetation areas (gardens, parks, garden squares) are clearly observed as the spots of lower temperature (Fig. 18f and Fig. 18h), in winter conditions it relates to the absence of anthropogenic sources of heat.

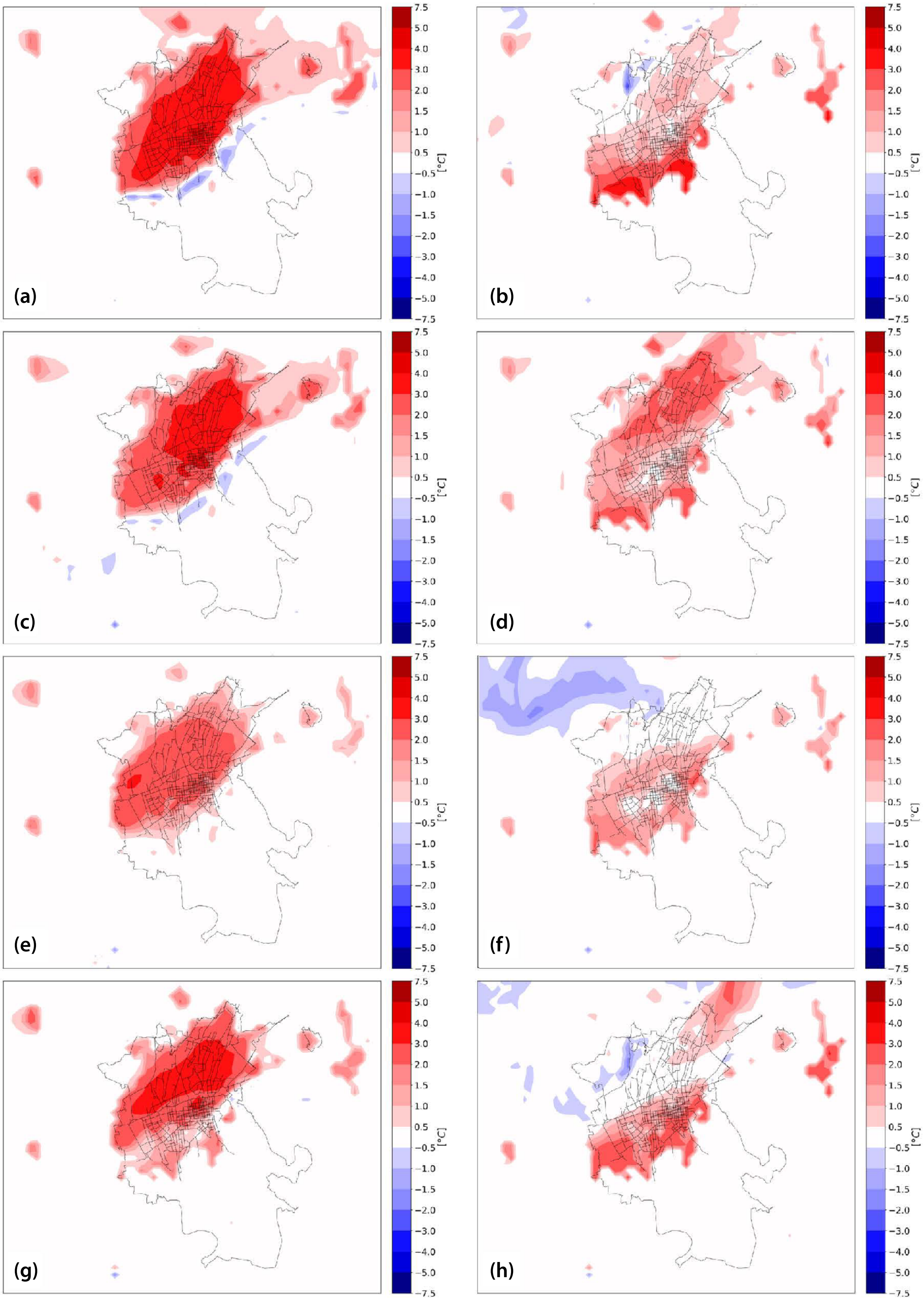

Fig. 18. Daylight (a, c, e, g) and nocturnal (b, d, f, h) heat islands for 4 days of anticyclone: 28.11, 29.11, 30.11 and 01.12.2016. Averaging time for daylight UHI from 11:00 through 16:00, for nocturnal - from 23:00 through 04:00.

CONCLUSION

This work discusses the tasks of modeling of the air basin of Almaty in stagnant environmentally unfavorable conditions by adjusting the WRF model to the complex rugged urban area. The zoning approach was used for a joint analysis of observation data and modeling results to solve the problems in connection with a sparse grid of meteorological stations. 4 climatic zones were identified (high mountain range, middle mountain range, the city and the steppe), each having one meteorological station. Based on the assumption that observation data for these meteorological stations characterize location zones, the following conclusions can be made:

1. The high mountain range is characterized by a high variety: a large wind velocity and temperature gradient. The simulations showed that the main impact of this zone on the underlying areas relates to the katabatic flow of cold air in the evening and night hours.
2. The interaction of the middle mountain range and the urban zone plays a key role in the formation of the city climate in synoptic conditions of the slow-moving atmospheric air. The anabatic airflow formed by noon, dies away in the middle mountain range due to the radiation heating of the slopes, oriented to the sun. Data of satellite survey and observations at the Kamenskoye Plato meteorological station show that in clear weather in the middle mountain range the ground and air next to the ground are heated by several degrees higher than the urban area.
3. The city zone is characterized by the heat island calculated in the work as a difference of temperature fields "with and without the city". The simulations showed that regularities of formation and development of heat islands for Almaty depend a lot on wind conditions. Especially it is prominent in the conditions of anticyclone where depending on the time of day, local winds suddenly change intensity and direction and thermal fields are changing simultaneously. E.g., unlike plain cities, the nocturnal heat island of Almaty is cooler than the daylight heat island due to the katabatic wind, which flows down in the evening and at night and diffuses in the urban quarters.
4. In general, the meteorological conditions of the northern steppe zone are formed by regional processes. Among them, there can be identified Shilik mountain breeze, forming in the gorge at the water heads of the Shilik River and spreading along the Ili valley. It reaches the northern suburbs of Almaty significantly weakened (up to 3–4 m/sec), but its energy is enough to form a more favorable climate.
5. As is known, mountain-valley wind circulation is followed by the formation and development of the inversion layer, and wind conditions in the surface layer has a cyclic nature with weak alternating up and down airflows. The results of modeling of these processes showed that surface inversion, formed by the nocturnal katabatic wind rises at daytime to an altitude of 150–200 m. In addition, in the layer between the surface and the lower border of inversion there forms daytime anabatic mountain breeze. At sunset, the cycle repeats. The simulations also revealed a wind damping effect in the urban area. In general, an unfavorable complex ecological picture of weak variable local winds with alternating calm and low-wind areas (1–2 m/sec) can be observed. The situation is aggravated by the inversion layer, which locks the vertical exchange, including turbulent diffusion of pollutants.
6. The results of modeling correlate well with the data of observation during the anticyclone period, however with the advent of warm intrusion simulation errors increase. In our perspective, these results confirm the previous study conclusions (Anthes *et al.*, 1985) that the numerical analysis of mesoscale and local processes can be prospectively applied to the situations where the impact of large-scale flows is minimal as compared to the processes generated by the heterogeneity of the underlying surface.
7. Prospects for the future development of this work lie in the field of air quality protection in the city of Almaty. It is planned to continue researches related to the modeling of transport and chemical transformation of pollutants (Zakarin *et al.*, 2021a) and designing the information system for analysis of risks of atmospheric pollution in case of variable location and capacity of the sources of emissions (Zakarin *et al.*, 2021b; Zakarin *et al.*, 2019).
8. For a rapidly developing Almaty, the task of expertise of the projects of development of new city areas is topical. For this purpose it is planned to use a procedure for modeling flows around urban buildings by coupling (Chen *et al.*, 2011) of the WRF mesoscale model with a small-scale CFD (Computational Fluid Dynamics) type of models, e.g., ENVI-met, or Urban Weather

Generator (UWG) (Bande *et al.*, 2019). Interaction of different-scale models suggests (i) a downscaling procedure, i.e. using modeling results on a coarse grid for the formation of initial and lateral boundary conditions of the small-scale model and (ii) an upscaling procedure, including parameterization of the processes in the urban canopy based on the modeling results on the fine grid.

9. For the development of climatically and environmentally safe, healthy and sustainable cities, subject to the recommendations of the World Meteorological Organization (WMO), further efforts are to be applied to the development of integrated urban hydro-meteorological, climate and environmental systems and services (WMO, 2019; Baklanov *et al.*, 2018). The target is to establish urban services meeting special needs of the cities, based on the combination of dense observation networks, high-resolution forecasts, multiple-hazard early warning systems, plans for natural hazard management and climatic services. Such approach provides the city with tools necessary to reduce emissions, to adopt to climate changes, to develop carbon neutral and environmentally comfortable cities, prosperous and sustainable societies and to implement UN Sustainable Development Goals.

CONFLICT OF INTEREST STATEMENT

The authors confirm the absence of the conflict of interest.

ACKNOWLEDGEMENT

This work has been prepared under the grant program of the Ministry of Education and Science of the Republic of Kazakhstan (No. AP05132380/GF).

REFERENCES

Akhmetzhanov, H.A., Shver, I.A. (1986) The climate of Alma-Ata. Hydrometizdat.

Anthes, R.A., Kuo, Y.H., Baumhefner, D.P., Errico, R.M., Bettge, T.W. (1985) Predictability of Mesoscale Atmospheric Motions. Advances in Geophysics, 28(PB), 159–202. https://doi.org/10.1016/S0065-2687(08)60188-0

Arnold, D., Morton, D., Schicker, I., Seibert, P., Rotach, M.W., Horvath, K., Dudhia, J., Satomura, T., Müller, M., Zängl, G., Takemi, T., Serafin, S., Schmidli, J., Schneider, S. (2012) High Resolution Modelling in Complex Terrain. Report on the HiRCoT 2012 Workshop, Vienna, 21–23 February 2012.

Baklanov, A., Grimmond, C.S.B., Carlson, D., Terblanche, D., Tang, X., Bouchet, V., Lee, B., Langendijk, G., Kolli, R.K., Hovsepyan, A. (2018) From urban meteorology, climate and environment research to integrated city services. Urban Climate, 23, 330–341. https://doi.org/10.1016/j.uclim.2017.05.004

Bande, L., Afshari, A., al Masri, D., Jha, M., Norford, L., Tsoupos, A., Marpu, P., Pasha, Y., Armstrong, P. (2019) Validation of UWG and ENVI-met models in an Abu Dhabi District, based on site measurements. Sustainability (Switzerland), 11(16), 4378. https://doi.org/10.3390/su11164378

Bao, J.-W., Michelson, S.A., Persson, P.O.G., Djalalova, I.v., Wilczak, J.M. (2008) Observed and WRF-Simulated Low-Level Winds in a High-Ozone Episode during the Central California Ozone Study. Journal of Applied Meteorology and Climatology, 47(9), 2372–2394. https://doi.org/10.1175/2008JAMC1822.1

Bougeault, P., Lacarrere, P. (1989) Parameterization of orography-induced turbulence in a mesobeta-scale model. Monthly Weather Review, 117(8), 1872–1890. https://doi.org/10.1175/1520-0493(1989)117<1872:POOITI>2.0.CO;2

Brousse, O., Martilli, A., Foley, M., Mills, G., Bechtel, B. (2016) WUDAPT, an efficient land use producing data tool for mesoscale models? Integration of urban LCZ in WRF over Madrid. Urban Climate, 17, 116–134. https://doi.org/10.1016/j.uclim.2016.04.001

Chen, F., Kusaka, H., Bornstein, R., Ching, J., Grimmond, C.S.B., Grossman-Clarke, S., Loridan, T., Manning, K.W., Martilli, A., Miao, S., Sailor, D., Salamanca, F.P., Taha, H., Tewari, M., Wang, X., Wyszogrodzki, A.A., Zhang, C. (2011) The integrated WRF/urban modelling system: development, evaluation, and applications to urban environmental problems. International Journal of Climatology, 31(2), 273–288. https://doi.org/10.1002/joc.2158

Diáz-Fernández, J., Quitián-Hernández, L., Bolgiani, P., Santos-Munõz, D., Garciá Gago, Á., Fernández-González, S., Valero, F., Merino, A., Garciá-Ortega, E., Sánchez, J.L., Sastre, M., Martín, M.L. (2020) Mountain Waves Analysis in the Vicinity of the Madrid-Barajas Airport Using the WRF Model. Advances in Meteorology, 2020, 887156. https://doi.org/10.1155/2020/8871546

Helmholtz, N.F. (1963) Mountain-valley circulation of the Tien Shan northern slopes. Hydrometizdat.

Iacono, M.J., Delamere, J.S., Mlawer, E.J., Shephard, M.W., Clough, S.A., Collins, W.D. (2008) Radiative forcing by long-lived greenhouse gases: Calculations with the AER radiative transfer models. Journal of Geophysical Research Atmospheres, 113(D13). https://doi.org/10.1029/2008JD009944

Isaev, E.K., Aniskina, O.G. (2015) The influence of parametrization schemes of microphysical processes on the quality of the forecast of atmospheric processes in an area with a complex relief by the example of the territory of Kyrgyzstan. Uchenye Zapiski RGGMU, 38, 118–125.

Isaev, E.K., Aniskina, O.G., Mostamandi, S.v. (2017) Evaluation of the effect of planetary boundary layer parametrizations in the WRF hydrodynamic model on the forecast quality of atmospheric processes in an area with a complex topography. Trudy GGO, 584, 123–141.

Isaev, E.K., Mostamandi, S.v., Aniskina, O.G. (2015) Evaluation of the influence of the parameterization of physical processes in the WRF hydrodynamic model on the quality of the forecast of atmospheric processes in an area with a complex topography using the example of the territory of Kyrgyzstan. Uchenye Zapiski RGGMU, 40, 30–41.

Jiménez, P.A., Dudhia, J. (2013) On the Ability of the WRF Model to Reproduce the Surface Wind Direction over Complex Terrain. Journal of Applied Meteorology and Climatology, 52(7), 1610–1617. https://doi.org/10.1175/JAMC-D-12-0266.1

Kain, J.S., Kain, J. (2004) The Kain - Fritsch convective parameterization: An update. Journal of Applied Meteorology, 43(1), 170–181. https://doi.org/10.1175/1520-0450(2004)043<0170:TKCPAU>2.0.CO;2

Kusaka, H., Kimura, F. (2004) Coupling a single-layer urban canopy model with a simple atmospheric model: Impact on urban heat island simulation for an idealized case. Journal of the Meteorological Society of Japan, 82(1), 67–80. https://doi.org/10.2151/jmsj.82.67

Lim, J.O.J., Hong, S.Y., Dudhia, J. (2004) The WRF-single-moment-microphysics scheme and its evaluation of the simulation of mesoscale convective systems. Bulletin of the American Meteorological Society.

Martilli, A., Clappier, A., Rotach, M.W. (2002) An urban surface exchange parameterisation for mesoscale models. Boundary-Layer Meteorology, 104, 261–304. https://doi.org/10.1023/A:1016099921195

Martilli, A., Clarke, S.G., Tewari, M., Manning, K.W. (2009) Description of the modification s made in WRF.3.1 and short user's manual of BEP. In NCAR.

Mauree, D., Blond, N., Clappier, A. (2018) Multi-scale modeling of the urban meteorology: Integration of a new canopy model in the WRF model. Urban Climate, 26, 60–75. https://doi.org/10.1016/j.uclim.2018.08.002

Michelson, S.A., Bao, J.W. (2008) Sensitivity of low-level winds simulated by the WRF model in California's Central Valley to uncertainties in the large-scale forcing and soil initialization. Journal of Applied Meteorology and Climatology, 47(12), 3131–3149. https://doi.org/10.1175/2008JAMC1782.1

Monin, A.S., Obukhov, A.M. (1954) Basic laws of turbulent mixing in the surface layer of the atmosphere. Contributions of the Geophysical Institute of the Academy of Sciences of the USSR.

Nehrkorn, T., Henderson, J., Leidner, M., Mountain, M., Eluszkiewicz, J., McKain, K., Wofsy, S. (2013) WRF Simulations of the Urban Circulation in the Salt Lake City Area for CO_2 Modeling. Journal of Applied Meteorology and Climatology, 52(2), 323–340. https://doi.org/10.1175/JAMC-D-12-061.1

Oke, T.R., Mills, G., Christen, A., Voogt, J.A. (2017) Urban climates. In Urban Climates. https://doi.org/10.1017/9781139016476

Segura, R., Badia, A., Ventura, S., Gilabert, J., Martilli, A., Villalba, G. (2021) Sensitivity study of PBL schemes and soil initialization using the WRF-BEP-BEM model over a Mediterranean coastal city. Urban Climate, 39, 100982. https://doi.org/10.1016/j.uclim.2021.100982

Siuta, D., West, G., Stull, R. (2017) WRF Hub-Height Wind Forecast Sensitivity to PBL Scheme, Grid Length, and Initial Condition Choice in Complex Terrain. Weather and Forecasting, 32(2), 493–509. https://doi.org/10.1175/WAF-D-16-0120.1

Skamarock, W.C., Klemp, J.B., Dudhia, J., Gill, D.O., Liu, Z., Berner, J., Wang, W., Powers, J.G., Duda, M.G., Barker, D.M., Huang, X.-Y. (2019) A Description of the Advanced Research WRF Model Version 4. https://library.ucar.edu/research/publish-technote

Vilesov, E.N. (2010) Climatic conditions of Almaty. Al-Farabi Kazakh National University Press.

Wilks, D.S. (2011) Time Series. International Geophysics, 100, 395–456. https://doi.org/10.1016/B978-0-12-385022-5.00009-9

WMO (World Meteorological Organization) (2019) Guidance on Integrated Urban Hydro-Meteorological, Climate and Environmental Services. In Urban Climate Science for Planning Healthy Cities: Vol. I (Issue 1234). https://library.wmo.int/doc_num.php?explnum_id=9903

Yáñez-Morroni, G., Gironás, J., Caneo, M., Delgado, R., Garreaud, R. (2018) Using the Weather Research and Forecasting (WRF) model for precipitation forecasting in an Andean region with complex topography. Atmosphere, 9(8), 304. https://doi.org/10.3390/atmos9080304

Zakarin, E.A., Baklanov, A.A., Balakay, L.A., Dedova, T.V., Bostanbekov, K.A. (2021) Simulation of Air Pollution in Almaty City under Adverse Weather Conditions. Russian Meteorology and Hydrology, 46(2), 121–128. https://doi.org/10.3103/S1068373921020072

Zakarin, E.A., Balakay, L.A., Bostanbekov, K.A., Dedova, T.V., Zhetpissov, R.A. (2019) Mathematical Modeling of the City Air Pollution Risks. Gidrometeorologiya i Ekologiya, 2(93), 50–62.

Zakarin, E.A., Dedova, T.V., Balakay, L.A., Bostanbekov, K.A. (2021) The technology of mapping the risks of atmospheric pollution by heat and power enterprises on the example of the city of Almaty. Ecology and Industry of Russia, 25(4). https://doi.org/10.18412/1816-0395-2021-4-21-27